Vital Surveillances

Evolutionary Diversity of Coxsackievirus A6 Causing Severe Hand, Foot, and Mouth Disease — China, 2012–2023

Huanhuan Lu[1]; Jinbo Xiao[1]; Wenhui Wang[2]; Dongmei Yan[1]; Tianjiao Ji[1]; Qian Yang[1]; Haiyan Wei[3]; Yanhua Du[4]; Yunting Zeng[5]; Jun Guo[6]; Jianhua Chen[7]; Hanri Zeng[8]; Yingying Liu[9]; Shuaifeng Zhou[10]; Hong Ji[11]; Jianxing Wang[12]; Xiaofang Zhou[13]; Yong Zhang[1,#]

ABSTRACT

Introduction: Coxsackievirus A6 (CVA6) has emerged as a significant pathogen responsible for severe cases of hand, foot, and mouth disease (HFMD). This study aims to delineate the demographic characteristics and analyze the viral evolution of severe HFMD associated with CVA6, thereby assisting in its surveillance and management.

Methods: In this investigation, 74 strains of CVA6 were isolated from samples collected from severe HFMD cases between 2012 and 2023. The *VP1* gene sequences of CVA6 were amplified and analyzed to assess population historical dynamics and evolutionary characteristics using BEAST, DnaSP6, and PopART.

Results: A significant portion (94.4%) of severe CVA6-associated HFMD cases (51 out of 54, with 20 lacking age information) were children under 5 years old. Among the 74 CVA6 strains analyzed, 72 belonged to the D3a sub-genotype, while only two strains were D2 sub-genotype. The average genetic distance between *VP1* sequences prior to 2015 was 0.027, which increased to 0.051 when compared to sequences post-2015. Historical population dynamics analysis indicated three significant population expansions of severe CVA6-associated HFMD during 2012–2013, 2013–2014, and 2019–2020, resulting in the formation of 65 distinct haplotypes. Consistent with the MCC tree findings, transitioning between regional haplotypes required multiple base substitutions, showcasing an increase in population diversity during the evolutionary process (from 14 haplotypes in 2013 to 55 haplotypes over the subsequent decade).

Conclusions: CVA6, associated with severe HFMD, is evolving and presents a risk of outbreak occurrence. Thus, enhanced surveillance of severe HFMD is imperative.

Hand, foot, and mouth disease (HFMD) is a contagious disease predominantly caused by several enteroviruses and primarily affects infants and children (*1*). Typically characterized by fever, mouth ulcers, and rash, HFMD symptoms are often mild and generally resolve within 7–10 days. However, some individuals may develop severe symptoms such as fever, a stiff neck, shortness of breath, and worsening rash, leading to potentially life-threatening neurological, respiratory, or circulatory complications, including aseptic meningitis, encephalitis, acute flaccid paralysis, pulmonary hemorrhage, pulmonary edema, and cardiopulmonary failure (*2*). HFMD was classified as a notifiable disease in May 2008, identifying enterovirus A71 (EV-A71) as the predominant pathogen responsible for severe and fatal cases (*3*). The widespread administration of an inactivated EV-A71 vaccine in 2016 significantly decreased the incidence of EV-A71-associated HFMD cases (*4*). Nevertheless, the diversity of pathogens leading to severe HFMD has evolved recently due to the absence of cross-protection among different enterovirus serotypes (*5*). Coxsackievirus A6 (CVA6) has emerged as the primary pathogen in severe HFMD cases across various regions in China. For instance, in 2013, the Third People's Hospital of Shenzhen reported that all eight patients with severe HFMD tested positive for CVA6, all developing meningitis, with two also suffering myocardial damage (*6*). Similarly, in 2017, the Guangdong Women and Children's Hospital found that among 55 patients with CVA6-associated severe HFMD, 29 (52.7%) developed aseptic meningitis, and six (10.9%) also experienced pulmonary edema (*7*).

Enteroviruses possess a single-stranded, positive-sense RNA genome that encodes both structural and nonstructural viral proteins. After entering a cell, the genomic RNA translates into a polyprotein divided

into three regions: P1, P2, and P3. This polyprotein is then segmented into individual proteins by viral proteases. Specifically, the P1 region comprises four structural proteins (*VP1*–*VP4*) (*8*). Variations in the nucleotide sequences of the *VP1* region are utilized for molecular typing of enteroviruses (*9*). Studies focusing on the molecular typing of CVA6 based on these sequences have identified the D3 sub-genotype as the predominant strain globally since 2008, with the D3a sub-genotype being the most widespread in China (*5*).

Based on the national laboratory surveillance network for HFMD pathogens established in the Chinese mainland in 2008, a total of 74 CVA6 strains were obtained from severe HFMD cases between 2012 and 2023. Analysis of their *VP1* sequences allowed for the inference of the population's historical dynamics and the evolutionary characteristics of CVA6. This study aims to provide insights into the surveillance of severe HFMD cases.

METHODS

Case Inclusion Criteria

According to the HFMD Treatment Guidelines (2010 and 2018 editions), severe HFMD cases were defined by the following clinical signs: persistent high fever (>39 °C), neurological symptoms (depression and abnormal movement), atypical respiratory symptoms (abnormalities in respiratory rate), and circulatory dysfunction (abnormal heart rate and prolonged capillary refill time). Cases that met these criteria were included in the study, which aimed to enhance public health surveillance and informed decision-making without involving human experimentation. The study received approval from the Second Ethics Review Committee of the National Institute for Viral Disease Control and Prevention at the Chinese Center for Disease Control and Prevention.

Sample Collection and Viral Isolation

According to surveillance guidelines, the local CDC collected samples (e.g., stool and throat swabs) from severe HFMD cases and transported them to designated laboratories for EVs screening using Real-time RT-PCR. All CVA6-positive samples were subsequently forwarded to the provincial CDC for virus isolation following the standard protocol (Polio Laboratory Manual, 4th ed, https://iris.who.int/handle/10665/68762). The National Polio Laboratory at the National Institute of Viral Disease Prevention and Control in China was tasked with genotype identification.

Molecular Typing of Enteroviruses

Nucleic acid extraction from cell cultures was carried out using the Tianlong nucleic acid extraction kit (Ex-DNA/RNA Virus (CDC)/T327, Xi'an Tianlong Technology Co., Ltd., China) and the GeneRotex 96 nucleic acid extractor (Xi'an Tianlong Technology Co., Ltd., China). The *VP1* coding region was amplified through reverse transcription polymerase chain reaction (RT-PCR) utilizing the PrimeScript One Step RT-PCR kit version 2 (RR057A, TaKaRa, China). Specific primers for amplification included CVA6-2339Y (5'–3': CCTTCTGAGGCCAACA TCAT) and CVA6-3461Z (5'–3': ATACCAAGTTGG CCCAGTCA). Sequencing was conducted using an ABI 3130 genetic analyzer (Applied Biosystems, Foster City, CA, USA), and data analysis was performed using Sequencher software (version 5.4.6, Ann Arbor, USA) to determine the *VP1* coding sequence of enteroviruses. Molecular typing of sequences was completed via the enterovirus typing tool available at www.rivm.nl/mpf/enterovirus/typingtool.

Inference of Population Historical Dynamics

The alignment of sequences was performed using MAFFT software (version 7.490) (*10*), while the best nucleotide substitution model was identified using ModelGenerator (version 0.85). RAxML-NG (version 0.9.0) was utilized to construct the maximum likelihood phylogenetic tree (*11*). TempEst (version 1.5) facilitated the analysis of the temporal structure of the sequences (*12*). The optimal molecular clock model and tree prior were determined through Path Sampling/Stepping-stone techniques (*13*). Bayesian phylogenetic analysis was executed using BEAST (version 1.8.4) (*14*), with the analysis outputs reviewed in Trace software (version 1.7.1). The Bayesian maximum clade credibility (MCC) tree was constructed using TreeAnnotator (version 1.8.4) and visualized in FigTree software (version 1.4) (http://tree.bio.ed.ac.uk/software/). A single haplotype was defined in DnaSP6 software (version 6.12.03) (*15*) when nucleotide sequences were identical, aiding in the understanding of nucleotide mutations throughout viral evolution. The median-joining haplotype network was built using PopART software (version 1.7).

RESULTS

Demographic Characteristics of HFMD Cases with CVA6 Infections

This study analyzed 74 CVA6 strains isolated from severe HFMD cases, which were submitted by provincial HFMD surveillance laboratories between 2012 and 2023. Of the 74 CVA6-associated severe HFMD cases, 48 were in males and 26 in females. The patients had a median age of 2.0 years (mean age 2.05 years, range 6 months to 6.5 years). The age distribution was as follows: 25 cases in children under 1 year old, 26 cases in those aged 1–5 years, and three cases in children older than 5 years (Table 1).

CVA6 isolates identified in 97.3% (72/74) of cases were predominantly of the D3a sub-genotype, while the D2 sub-genotype was solely found in Northwest China (Figure 1). The cases were primarily located in Central and Western China, with the most cases reported in Northwest China (25 cases), followed by Central China (22 cases), South China (13 cases), Southwest China (8 cases), North China (4 cases), and East China (2 cases). Incidences before 2015 were predominantly in Northwest China, whereas occurrences post-2015 were mainly in Central, South, and Southwest China (Table 1).

Inference of Population Historical Dynamics

The MCC tree analysis revealed that CVA6 sequences from the same geographical region displayed high similarity and often clustered together. Regarding the temporal distribution of CVA6 in severe HFMD cases, sampling in Northwest China was primarily conducted before 2015. In contrast, post-2015 samples predominantly came from patients with severe HFMD in Central, South, and Southwest China. The evolutionary distances between post-2015 sequences and those isolated earlier in Northwest China significantly increased. Specifically, the average genetic distance was 0.027 for sequences before 2015 and increased to 0.051 for sequences post-2015 compared to earlier sequences (Figure 2A). Within the same region, the average genetic distance among sequences was 0.032, whereas it was 0.044 between different regions (Figure 2B). Furthermore, Bayesian skyline plot analysis indicated that the D3a sub-genotype of CVA6, isolated from 72 cases, experienced three population expansions during its evolutionary history, specifically in 2012–2013, 2013–2014, and 2019–2020. Notably, there were significant increases in the population size during the periods 2012–2013 and 2019–2020 (Figure 2C).

Analysis of the 72 CVA6 D3a *VP1* sequences identified 258 variable sites within the 915 bp fragment, encompassing 65 haplotypes. In 2013, there were 14 haplotypes, with 41 additional haplotypes emerging over the subsequent decade. Of the 65 haplotypes, 58 (89.2%, 58/65) comprised solely a single sequence. These haplotypes were distributed across various regions, forming several large clusters of regionally originated haplotypes in the haplotype network plot and the MCC tree. This clustering indicates that haplotypes from different regions diverged through multiple base substitutions. The analyses also imply the existence of further undetected samples, as evidenced in Figure 2D and Table 1.

DISCUSSION

Unlike mild HFMD, severe cases can lead to neurological, respiratory, or circulatory complications, and treatment delays may result in further deterioration. EV-A71 has been identified as the predominant pathogen responsible for severe HFMD. However, following the introduction of the inactivated EV-A71 vaccine in 2016, the spectrum of pathogens causing HFMD has shifted, with other enteroviruses, particularly CVA6, emerging as the primary causative agents (*5*).

Seventy-four cases of severe HFMD associated with CVA6 were reported in children under the age of 5 years. The immature immune systems of this age group may heighten their susceptibility, leading to severe complications and potentially fatal outcomes if not promptly diagnosed and treated (*2*). Consequently, the development and administration of vaccines targeting CVA6 are crucial to prevent severe HFMD in susceptible children.

The CVA6 genotype, particularly the dominant D3a sub-genotype in China, has been isolated primarily, with only two instances of the D2 strain identified in 2013. This underscores the necessity for ongoing robust surveillance of severe HFMD specifically targeting the CVA6 D3a sub-genotype. In this study, a total of 74 CVA6 strains were collected from severe HFMD cases between 2012 and 2023, predominantly in Central China, Northwest China, and South China. It is important to note that the limited number of samples and the considerable variability in surveillance quality across provinces may introduce bias in the

TABLE 1. Summary of information on 74 cases of CVA6-associated severe hand, foot, and mouth disease in China, 2012–2023.

Patient number	Gender	Age (years)	Region	Year	Haplotype	Sub-genotype	NMDC number
HFMD1	Female	1	Northwest China	2018	Hap_41	D3a	NMDCN00038LF
HFMD2	Male	1	Northwest China	2017	Hap_37	D3a	NMDCN00038L8
HFMD3	Female	2	Northwest China	2015	Hap_42	D3a	NMDCN00038LI
HFMD4	Male	4	Northwest China	2015	Hap_43	D3a	NMDCN00038LJ
HFMD5	Female	3	Northwest China	2015	Hap_29	D3a	NMDCN00038JS
HFMD6	Female	1	South China	2021	Hap_48	D3a	NMDCN00038K8
HFMD7	Male	2	South China	2023	Hap_56	D3a	NMDCN00038LH
HFMD8	Female	2	South China	2023	Hap_57	D3a	NMDCN00038LN
HFMD9	Male	2	South China	2023	Hap_58	D3a	NMDCN00038LQ
HFMD10	Male	4	South China	2020	Hap_47	D3a	NMDCN00038K5
HFMD11	Male	2	Southwest China	2022	Hap_62	D3a	NMDCN00038LU
HFMD12	Male	4	Southwest China	2022	Hap_63	D3a	NMDCN00038LV
HFMD13	Male	4	Southwest China	2022	Hap_63	D3a	NMDCN00038M0
HFMD14	Male	3	Southwest China	2022	Hap_64	D3a	NMDCN00038M1
HFMD15	Female	1	Southwest China	2022	Hap_60	D3a	NMDCN00038LR
HFMD16	Male	2	Southwest China	2022	Hap_61	D3a	NMDCN00038LS
HFMD17	Female	2	Southwest China	2020	Hap_59	D3a	NMDCN00038LC
HFMD18	Female	5	South China	2018	Hap_54	D3a	NMDCN00038KS
HFMD19	Female	< 1	South China	2018	Hap_55	D3a	NMDCN00038KT
HFMD20	Female	2	South China	2018	Hap_55	D3a	NMDCN00038KU
HFMD21	Male	1	South China	2018	Hap_53	D3a	NMDCN00038KR
HFMD22	Female	2	South China	2018	Hap_51	D3a	NMDCN00038KM
HFMD23	Female	1	South China	2018	Hap_52	D3a	NMDCN00038KN
HFMD24	Male	5	South China	2018	Hap_49	D3a	NMDCN00038KK
HFMD25	Male	2	South China	2018	Hap_50	D3a	NMDCN00038KL
HFMD26	Male	< 1	North China	2017	Hap_25	D3a	NMDCN00038KO
HFMD27	Female	< 1	North China	2017	Hap_26	D3a	NMDCN00038KQ
HFMD28	Male	2	North China	2017	Hap_24	D3a	NMDCN00038KJ
HFMD29	Male	1	North China	2015	Hap_23	D3a	NMDCN00038K2
HFMD30	Male	1	Central China	2019	Hap_14	D3a	NMDCN00038L3
HFMD31	Male	/*	Central China	2020	Hap_6	D3a	NMDCN00038K3
HFMD32	Female	−	Central China	2020	Hap_12	D3a	NMDCN00038L0
HFMD33	Male	−	Central China	2020	Hap_9	D3a	NMDCN00038KB
HFMD34	Male	−	Central China	2020	Hap_10	D3a	NMDCN00038KC
HFMD35	Male	−	Central China	2020	Hap_11	D3a	NMDCN00038KP
HFMD36	Female	−	Central China	2020	Hap_3	D3a	NMDCN00038JU
HFMD37	Male	−	Central China	2020	Hap_4	D3a	NMDCN00038JV
HFMD38	Male	−	Central China	2020	Hap_5	D3a	NMDCN00038K1
HFMD39	Male	−	Central China	2020	Hap_7	D3a	NMDCN00038K4
HFMD40	Male	−	Central China	2020	Hap_7	D3a	NMDCN00038K6
HFMD41	Male	−	Central China	2020	Hap_8	D3a	NMDCN00038K9
HFMD42	Male	−	Central China	2020	Hap_1	D3a	NMDCN00038JR

Continued

Patient number	Gender	Age (years)	Region	Year	Haplotype	Sub-genotype	NMDC number
HFMD43	Male	–	Central China	2020	Hap_15	D3a	NMDCN00038L4
HFMD44	Male	–	Central China	2020	Hap_17	D3a	NMDCN00038L9
HFMD45	Male	–	Central China	2020	Hap_18	D3a	NMDCN00038LD
HFMD46	Male	–	Central China	2020	Hap_19	D3a	NMDCN00038LG
HFMD47	Female	–	Central China	2020	Hap_20	D3a	NMDCN00038LK
HFMD48	Female	–	Central China	2020	Hap_20	D3a	NMDCN00038LO
HFMD49	Male	–	Central China	2020	Hap_13	D3a	NMDCN00038L1
HFMD50	Female	6	Central China	2019	Hap_16	D3a	NMDCN00038L6
HFMD51	Male	4	Central China	2014	Hap_2	D3a	NMDCN00038JT
HFMD52	Male	4	East China	2017	Hap_21	D3a	NMDCN00038L7
HFMD53	Female	1	East China	2017	Hap_22	D3a	NMDCN00038LT
HFMD54	Female	3	Northwest China	2020	Hap_32	D3a	NMDCN00038KE
HFMD55	Male	4	Northwest China	2020	Hap_33	D3a	NMDCN00038KF
HFMD56	Male	<1	Northwest China	2013	Hap_35	D3a	NMDCN00038KH
HFMD57	Male	1	Northwest China	2013	Hap_45	D3a	NMDCN00038LM
HFMD58	Female	3	Northwest China	2013	Hap_39	D3a	NMDCN00038LB
HFMD59	Female	1	Northwest China	2013	Hap_36	D3a	NMDCN00038KI
HFMD60	Male	1	Northwest China	2013	Hap_32	D3a	NMDCN00038KD
HFMD61	Male	1	Northwest China	2013	Hap_31	D3a	NMDCN00038K7
HFMD62	Female	1	Northwest China	2013	Hap_30	D3a	NMDCN00038K0
HFMD63	Female	2	Northwest China	2013	Hap_46	D3a	NMDCN00038LP
HFMD64	Male	1	Northwest China	2013	Hap_44	D3a	NMDCN00038LL
HFMD65	Male	1	Northwest China	2013	Hap_40	D3a	NMDCN00038LE
HFMD66	Male	2	Northwest China	2013	Hap_38	D3a	NMDCN00038LA
HFMD67	Male	1	Northwest China	2013	Hap_37	D3a	NMDCN00038L5
HFMD68	Male	2	Northwest China	2013	Hap_34	D3a	NMDCN00038KG
HFMD69	Male	1	Northwest China	2013	/†	D2	NMDCN00038KA
HFMD70	Male	1	Northwest China	2013	–	D2	NMDCN00038L2
HFMD71	Male	1	Northwest China	2013	Hap_27	D3a	NMDCN00038JP
HFMD72	Female	1	Northwest China	2014	Hap_36	D3a	NMDCN00038KV
HFMD73	Female	2	Northwest China	2014	Hap_28	D3a	NMDCN00038JQ
HFMD74	Male	–	Southwest China	2021	Hap_65	D3a	NMDCN00038M2

Note: Northwest China includes Shaanxi, Gansu, and Qinghai provinces; and Ningxia Hui Autonomous Region and Xinjiang Uygur Autonomous Region. South China includes Guangdong and Hainan provinces; Guangxi Zhuang Autonomous Region; and Hong Kong SAR and Macao SAR. Southwest China includes Sichuan, Guizhou, and Yunnan provinces; Chongqing Municipality; and Xizang Autonomous Region. North China includes Hebei and Shanxi provinces; Beijing and Tianjin Municipality; and Inner Mongolia Autonomous Region. Central China includes Henan, Hubei, and Hunan provinces. East China includes Jiangsu, Zhejiang, Anhui, Fujian, Jiangxi, and Shandong provinces; Shanghai Municipality; and Taiwan, China.
Abbreviation: HFMD=hand, foot and mouth disease; SAR=Special Administrative Region.
* Missing age information for this case;
† No haplotype analysis of D2.

analysis, potentially skewing the true prevalence of CVA6-associated severe HFMD.

D3a has been the predominant sub-genotype of CVA6 in China since 2012. Population dynamic analyses reveal that the virus isolated from severe HFMD cases exhibited three major expansions, reflecting increased diversity within the CVA6 population post-2012. Haplotype reconstruction from 74 sequences identified 65 unique haplotypes, underscoring the extensive diversity among CVA6

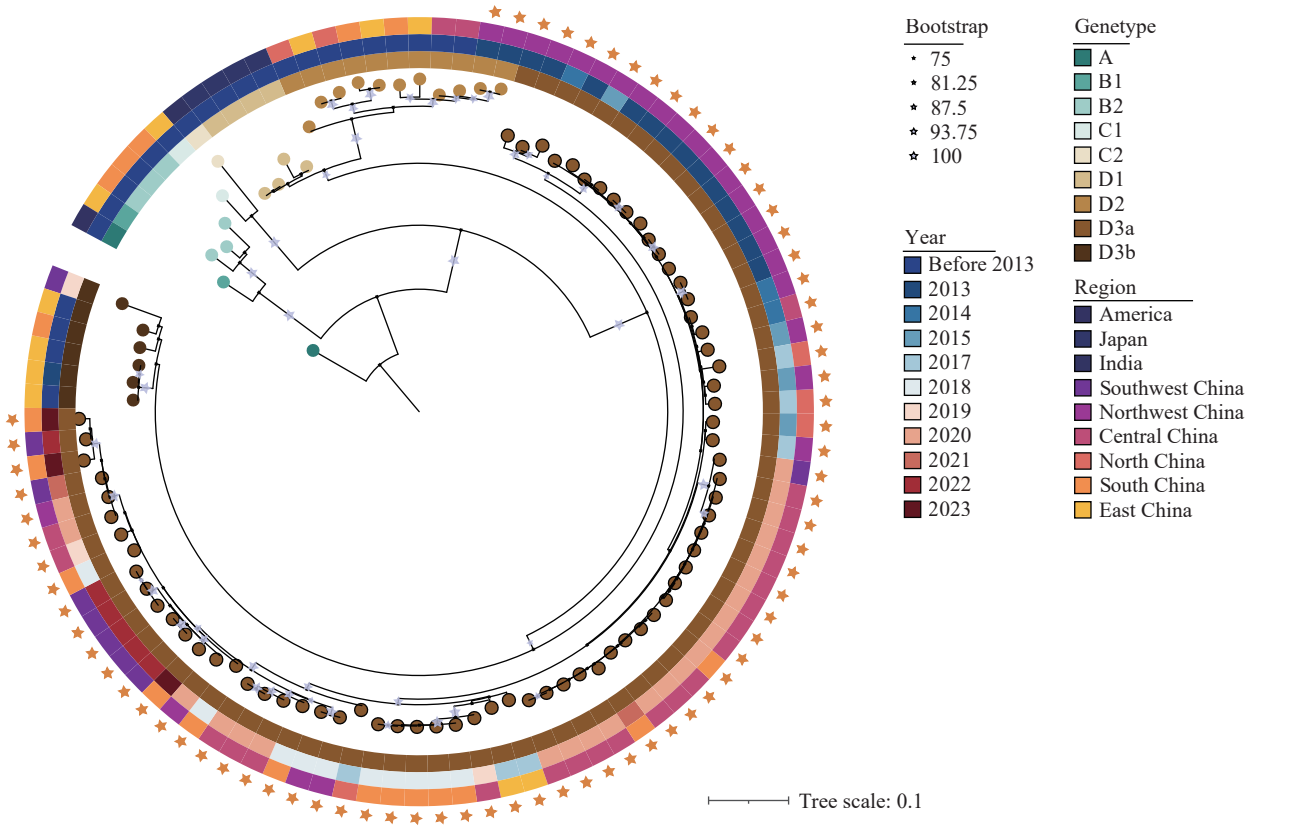

FIGURE 1. Molecular typing of 74 CVA6 strains isolated from severe HFMD in China, 2012–2023. The ML tree, constructed using the VP1 coding region, was utilized to determine the genotype of the CVA6 strains isolated in this study.
Abbreviation: CVA6=Coxsackievirus A6; HFMD=hand, foot, and mouth disease; ML=maximum likelihood.

strains associated with severe HFMD across different regions. Notably, no shared haplotypes were found between regions, suggesting the existence of undetected haplotypes and potentially unmonitored severe HFMD cases associated with CVA6. Current diagnostic criteria for severe HFMD, which include mild clinical symptoms with neurological or circulatory complications (*2*), may lead to misdiagnoses, such as enteroviral meningitis, thus contributing to the underreporting of severe HFMD cases. Given these findings, enhancing surveillance and improving clinician training on the identification and reporting of severe HFMD is essential to better assess and manage the disease burden.

Conflicts of interest: No conflicts of interest.

Acknowledgements: The staff of the local Centers for Disease Control and Prevention in Gansu, Guangdong, Guizhou, Hainan, Hebei, Henan, Hunan, Jiangsu, Shandong, Shaanxi, Sichuan, Yunnan, Zhejiang, and Chongqing PLADs for their efforts in collecting the clinical samples.

Funding: Supported by the Beijing Natural Science Foundation (L234052) and the National Key Research and Development Program of China (2021YFC2302003).

doi: 10.46234/ccdcw2024.086

Corresponding author: Yong Zhang, yongzhang75@sina.com.

[1] National Key Laboratory of Intelligent Tracking and Forecasting for Infectious Diseases; World Health Organization Polio Reference Laboratory for the Western Pacific Region; Key Laboratory of Laboratory Biosafety, National Health and Key Laboratory of Laboratory Biosafety of the National Health Commission, National Institute for Viral Disease Control and Prevention, Chinese Center for Disease Control and Prevention, Beijing, China; [2] Linyi Center for Disease Control and Prevention, Linyi City, Shandong Province, China; [3] Henan Provincial Center for Disease Control and Prevention, Zhengzhou City, Henan Province, China; [4] Shaanxi Provincial Center for Disease Control and Prevention, Xi'an City, Shaanxi Province, China; [5] Hainan Provincial Center for Disease Control and Prevention, Haikou City, Hainan Province, China; [6] Guizhou Provincial Center for Disease Control and Prevention, Guiyang City, Guizhou Province, China; [7] Gansu Provincial Center for Disease Control and Prevention, Lanzhou City, Gansu Province, China; [8] Guangdong Provincial Center for Disease Control and Prevention, Guangzhou City, Guangdong Province, China; [9] Hebei Provincial Center for Disease Control and Prevention, Shijiazhuang City, Hebei Province, China; [10] Hunan Provincial Center for Disease Control and Prevention, Changsha City, Hunan Province, China; [11] Jiangsu Provincial Center for Disease Control and Prevention, Nanjing City, Jiangsu Province, China; [12] Shandong Provincial Center for Disease Control and Prevention, Jinan City, Shandong Province, China; [13] Yunnan Provincial Center for Disease Control and Prevention, Kunming City, Yunnan Province, China.

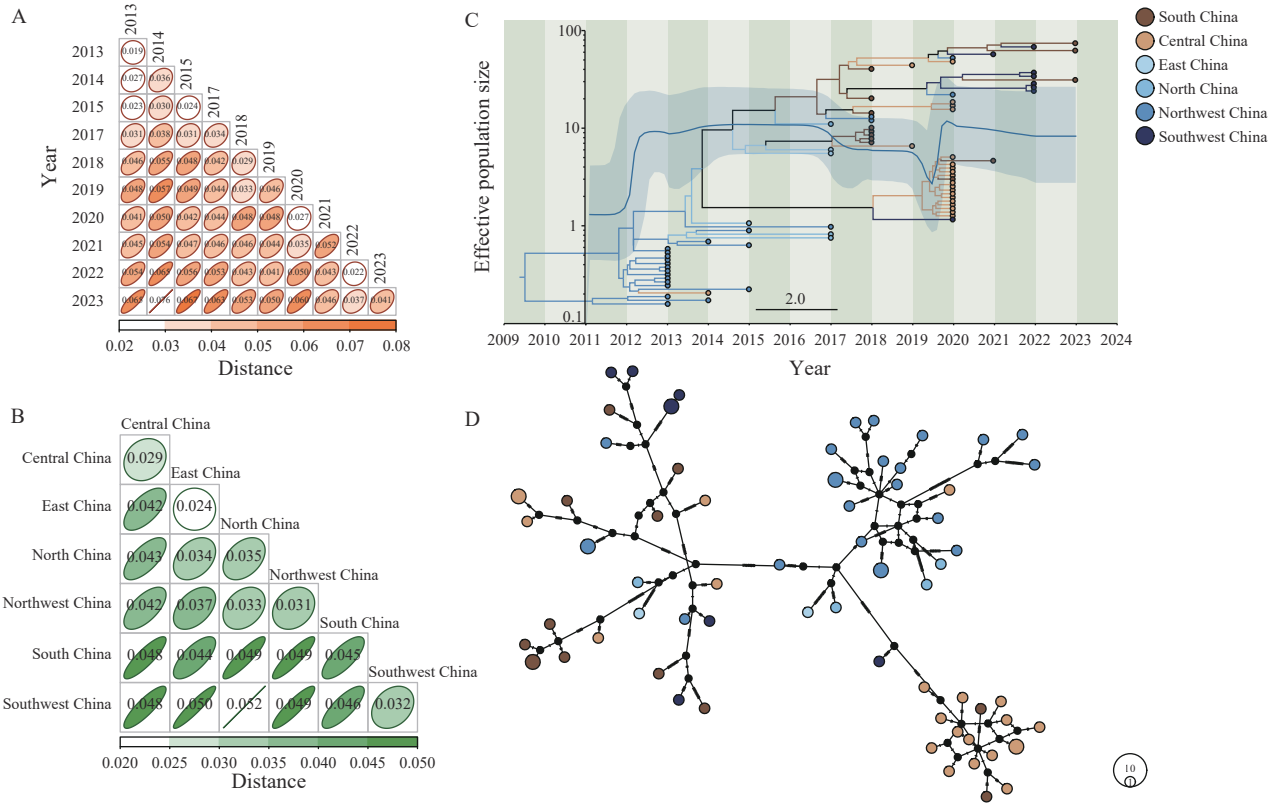

FIGURE 2. Inferred historical population dynamics of 74 CVA6 strains isolated from severe HFMD cases in China, 2012–2023. (A) Variation in nucleotide sequences of CVA6 from different regions. (B) Variation in nucleotide sequences of CVA6 across different years. (C) MCC tree and Bayesian skyline plot of the VP1 region of CVA6 depicting the 95% confidence intervals of the HPD analysis with light blue shading. Sequences from various regions are differentiated by color. (D) In the median-joining network, the circle size correlates with haplotype frequency, while unsampled haplotypes are shown as small black solid circles. Each connecting line indicates a mutational step between haplotypes.
Abbreviation: CVA6=Coxsackievirus A6; HFMD=Hand, foot, and mouth disease; MCC=Maximum clade credibility; HPD=Highest posterior density.

Submitted: February 02, 2024; Accepted: May 08, 2024

REFERENCES

1. Xu W, Liu CF, Yan L, Li JJ, Wang LJ, Qi Y, et al. Distribution of enteroviruses in hospitalized children with hand, foot and mouth disease and relationship between pathogens and nervous system complications. Virol J 2012;9:8. https://doi.org/10.1186/1743-422x-9-8.
2. Chong CY, Chan KP, Shah VA, Ng WYM, Lau G, Teo TES, et al. Hand, foot and mouth disease in Singapore: a comparison of fatal and non-fatal cases. Acta Paediatr 2003;92(10):1163-9.
3. Tan XJ, Huang XY, Zhu SL, Chen H, Yu QL, Wang HY, et al. The persistent circulation of enterovirus 71 in People's Republic of China: causing emerging nationwide epidemics since 2008. PLoS One 2011;6(9):e25662. https://doi.org/10.1371/journal.pone.0025662.
4. Xiao JB, Huang KQ, Lu HH, Song Y, Han ZZ, Zhang M, et al. Genomic epidemiology and phylodynamic analysis of enterovirus A71 reveal its transmission dynamics in Asia. Microbiol Spectr 2022;10(5):e0195822. https://doi.org/10.1128/spectrum.01958-22.
5. Song Y, Zhang Y, Han ZZ, Xu W, Xiao JB, Wang XJ, et al. Genetic recombination in fast-spreading coxsackievirus A6 variants: a potential role in evolution and pathogenicity. Virus Evol 2020;6(2):veaa048. https://doi.org/10.1093/ve/veaa048.
6. Yang F, Yuan J, Wang X, Li J, Du J, Su H, et al. Severe hand, foot, and mouth disease and coxsackievirus A6-Shenzhen, China. Clin Infect Dis 2014;59(10):1504 – 5. https://doi.org/10.1093/cid/ciu624.
7. Yang XH, Li YY, Zhang CB, Zhan WL, Xie J, Hu SQ, et al. Clinical features and phylogenetic analysis of severe hand-foot-and-mouth disease caused by Coxsackievirus A6. Infect Genet Evol 2020;77:104054. https://doi.org/10.1016/j.meegid.2019.104054.
8. Zhang Y, Hong M, Sun Q, Zhu SL, Tsewang N, Li XL, et al. Molecular typing and characterization of a new serotype of human enterovirus (EV-B111) identified in China. Virus Res 2014;183:75 – 80. https://doi.org/10.1016/j.virusres.2014.01.002.
9. Oberste MS, Maher K, Kilpatrick DR, Pallansch MA. Molecular evolution of the human enteroviruses: correlation of serotype with VP1 sequence and application to picornavirus classification. J Virol 1999;73(3):1941 – 8. https://doi.org/10.1128/jvi.73.3.1941-1948.1999.
10. Katoh K, Rozewicki J, Yamada KD. MAFFT online service: multiple sequence alignment, interactive sequence choice and visualization. Brief Bioinform 2019;20(4):1160 – 6. https://doi.org/10.1093/bib/bbx108.
11. Kozlov AM, Darriba D, Flouri T, Morel B, Stamatakis A. RAxML-NG: a fast, scalable and user-friendly tool for maximum likelihood phylogenetic inference. Bioinformatics 2019;35(21):4453 – 5. https://doi.org/10.1093/bioinformatics/btz305.
12. Rambaut A, Lam TT, Max Carvalho L, Pybus OG. Exploring the temporal structure of heterochronous sequences using TempEst (formerly Path-O-Gen). Virus Evol 2016;2(1):vew007. https://doi.org/10.1093/ve/vew007.
13. Baele G, Lemey P, Bedford T, Rambaut A, Suchard MA, Alekseyenko

AV. Improving the accuracy of demographic and molecular clock model comparison while accommodating phylogenetic uncertainty. Mol Biol Evol 2012;29(9):2157 – 67. https://doi.org/10.1093/molbev/mss084.
14. Drummond AJ, Suchard MA, Xie D, Rambaut A. Bayesian phylogenetics with BEAUti and the BEAST 1. 7. Mol Biol Evol 2012;29(8):1969 – 73. https://doi.org/10.1093/molbev/mss075.
15. Rozas J, Ferrer-Mata A, Sánchez-DelBarrio JC, Guirao-Rico S, Librado P, Ramos-Onsins SE, et al. DnaSP 6: DNA sequence polymorphism analysis of large data sets. Mol Biol Evol 2017;34(12):3299 – 302. https://doi.org/10.1093/molbev/msx248.